PROCEEDINGS OF SPIE

SPIEDigitalLibrary.org/conference-proceedings-of-spie

Fusing acoustic and optical sensing for needle tracking with ultrasound

Alexis Cheng, Bofeng Zhang, Philip Oh, Emad M. Boctor

Alexis Cheng, Bofeng Zhang, Philip Oh, Emad M. Boctor, "Fusing acoustic and optical sensing for needle tracking with ultrasound," Proc. SPIE 10576, Medical Imaging 2018: Image-Guided Procedures, Robotic Interventions, and Modeling, 105762I (13 March 2018); doi: 10.1117/12.2297644

SPIE.

Event: SPIE Medical Imaging, 2018, Houston, Texas, United States

Fusing acoustic and optical sensing for needle tracking with ultrasound

Alexis Cheng[a], Bofeng Zhang[b], Phillip Oh[b], Emad M. Boctor[a,c,d]

[a]Dept. of Computer Science, Johns Hopkins University, Baltimore, MD, USA
[b]Dept. of Biomedical Engineering, Johns Hopkins University, Baltimore, MD, USA
[c]Dept. of Electrical Engineering, Johns Hopkins University, Baltimore, MD, USA
[d]Dept. of Radiology, Johns Hopkins University, Baltimore, MD, USA

Abstract

Needles are used in many surgical procedures such as drug delivery or needle biopsies. One of the key challenges when using needles in these interventions is the placement of the needle. Placement of the needle at the goal position will ensure proper execution of the surgical plan as well as avoid possible complications. This work explores tracking a needle with a piezoelectric sensor embedded at its tip with an ultrasound transducer and a mono-camera. While each of the ultrasound transducer and the mono-camera sensors are insufficient on their own, one can uniquely locate the position of the piezoelectric sensor by combining these two sources of sensor information together. The information from each sensor can be processed to determine a geometrical locus on which the piezoelectric sensor must lie. By spatially combining the geometrical loci from the two sensors using an ultrasound calibration process, one can uniquely determine the location of the piezoelectric sensor. An experiment in a water tank was conducted with the computed results compared to ground truth cartesian stage data. An in-plane accuracy measure resulted in errors of 0.63mm and 0.18mm. The relative accuracy measure had a minimum, maximum, mean, and standard deviation of 0.02mm, 2.15mm, 0.61mm, and 0.61mm respectively. Future work will focus on demonstrating this method in more realistic *ex vivo* scenarios and explore whether our listed assumptions hold.

1. Introduction

Needles are used in many surgical procedures such as drug delivery or needle biopsies. One of the key challenges when using needles in these interventions is the placement of the needle. Placement of the needle at the goal position will ensure proper execution of the surgical plan as well as avoid possible complications.

The tracking of needles, will generally make use of external tracking sensors such as optical tracking or electromagnetic (EM) sensing [1] to provide real time spatial information of the tool relative to the patient. Optical tracking systems require line of sight, while EM-based systems are wired and subject to EM field distortions, discouraging the use of metallic tools. In addition, the estimation of the tool tips is limited by tool shaft bending and the effects of angle estimation error if the sensors themselves are placed far away from the tip. Further, IOUS to camera or IOUS to tool tracking transformations necessarily require an indirect calculation based on a chain of spatial transformations, each with errors that may propagate to the next. The tools themselves are also often difficult to visualize within an IOUS image. Stoll et al. [2] attached passive markers on the surgical instrument such that its position and orientation could be

Medical Imaging 2018: Image-Guided Procedures, Robotic Interventions, and Modeling, edited by Baowei Fei, Robert J. Webster III, Proc. of SPIE Vol. 10576, 105762I · © 2018 SPIE
CCC code: 1605-7422/18/$18 · doi: 10.1117/12.2297644

determined from an ultrasound image. Okazawa et al. and Cheung et al. explored image processing [3] and beamforming approaches [4] to enhance tool visibility.

This work explores the use of a needle with a piezoelectric (PZT) sensor embedded at its tip. Like the work presented by Guo et al. [5], this can aid in visualization and detection of the needle tip within an ultrasound image. This sensor is insufficient for three-dimensional tracking by itself. Thus, a mono-camera is attached to the ultrasound transducer. On its own, it is also insufficient, but we show in this work how one can combine these two sources of sensor information to enable three-dimensional tracking of the needle tip.

2. Technical Approach

2.1 Mono-camera needle segmentation and processing

Needle segmentation from camera images is required to obtain half of the necessary information to localize the needle tip. The needle appears as a line in the camera image. Since we are working with a single camera, the location of this needle is under-determined. The three-dimensional physical location of each image point observed by a single camera can be modeled as a line extending from the camera's optical center through this point in the image with depth uncertainty. Thus, if we extend this to every point on the needle, we end up with a plane spanning each of these lines on which the needle must lie on in three-dimensional space.

To segment the needle, we use a three-step approach. First, we apply an intensity filter across the image to reduce the background of the image. Then, we apply a Hough transform [6] to determine the locations of lines within the image. Finally, we apply a line length filter to only keep the longest, most well-defined set of lines. These set of lines typically include either edge of the needle and can then be averaged together to obtain the needle centerline. We can then determine the plane on which the needle lies on by picking any two points, p_1 and p_2, on the segmented needle centerline. Referring to equation 1 where o is the camera's optical center, we can define the plane by its normal, N, and vector, v. This plane will be used later when we fuse it with the ultrasound information to obtain the needle tip position.

$$\begin{gathered} N = (p_1 - o)x(p_2 - o) \\ v = p_1 - o \end{gathered} \tag{1}$$

2.2 Ultrasound signal segmentation and processing

The piezoelectric element acts as an active acoustic source and we model it as an ideal point source. One important note is that active point sources can be observed in the ultrasound image even if it is outside of the imaging plane. Active point sources are generally straight-forward to segment from ultrasound images because they either have higher intensity than the background or the ultrasound system can be configured such that there is no acoustic transmission and hence no background. In this case, we use an intensity filter to determine the location of the active point as observed in the ultrasound image.

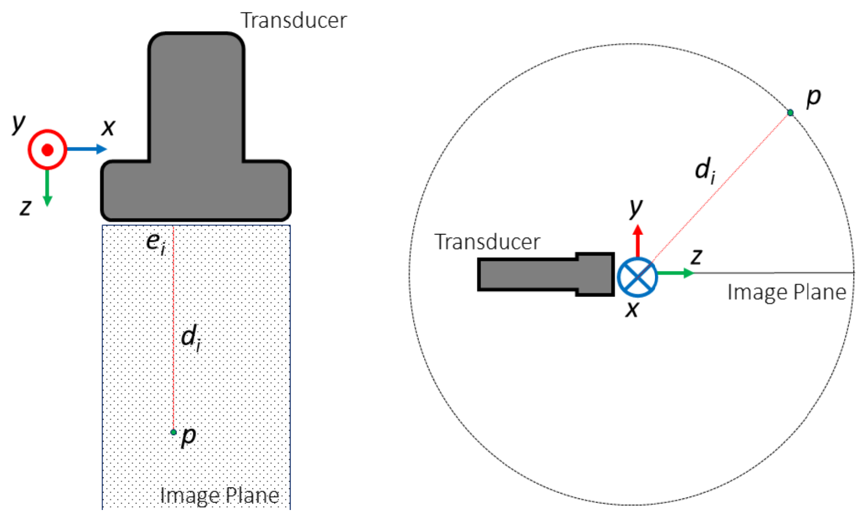

Figure 1. Out-of-plane estimation. Given the lateral coordinate and the distance between the point and the transducer element closest to it, the point must exist on a circle within the axial-elevational plane. [7]

We use the same out-of-plane estimation described previously in our active point calibration work [7]. This circular arc, C, can be parametrized as shown in equation 2, which will allow it to be easily transformed to another coordinate system. In this equation, e_i refers to the lateral position of the segmented piezoelectric signal and d_i refers to its axial position. t is then the parametrized angle defining the rotation of this point about the ultrasound transducer's lateral axis.

$$\forall t = -90^o : 90^o : C(t) = \begin{bmatrix} e_i \\ d_i \sin(t) \\ d_i \cos(t) \end{bmatrix} \tag{2}$$

2.3 Camera and ultrasound sensor fusion

The information obtained by each of the individual sensors can only incompletely determine the position of the needle. However, they compensate for each other when combined. The first step to combining the information from these two sensors is to put them in the same coordinate system. The plane is originally defined with respect to the camera, while the arc is defined with respect to the ultrasound transducer. Thus, one way of relating these two coordinate systems is through an ultrasound calibration process. There are many possible calibration methods. We used the active calibration phantom [7].

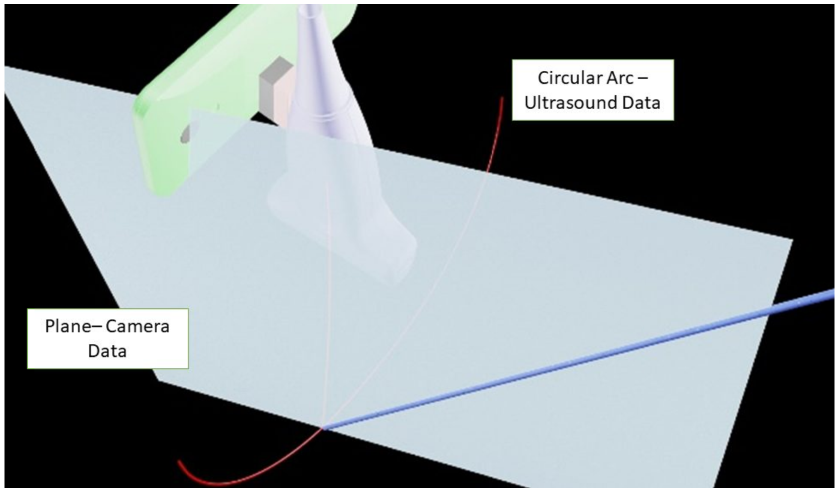

Figure 2. Graphical representation of intersection between plane acquired from the camera and circular arc acquired from the ultrasound probe.

After the information from these two coordinate systems are calibrated such that they are within the same coordinate system, one can then fuse the information together to localize the position of the needle tip. Since the information from each sensor constrains the location of the needle tip to some set of possible locations, their intersection will result in the needle tip's location. Figure 2 shows the intersection of the information from these two sensors graphically. Equation 3 describes this relationship analytically, where X is the calibration transforming every ultrasound point into the camera frame. This relationship is only satisfied when $X * C(t)$ lies on the camera and needle plane.

$$(X * C(t) - o) \cdot N = 0 \tag{3}$$

3. Experiments

In these experiments, the piezoelectric element is fixed to the end of a rigid tube to emulate a the element being placed at the end of a needle tip. Two experiments were performed to evaluate this needle tracking approach. The first involves placing the piezoelectric element at the needle tip inside of the ultrasound imaging plane. We then compare the computed position with where it appears to be in the image. As shown in figure 3, the second experimental setup consists of moving the ultrasound transducer with a Cartesian stage to a set of known locations. The piezoelectric element is then localized at each of these independent locations. We use the relative accuracy measure described in equation 4 to validate this method. N is the number of total data points (50). q is the localized piezoelectric element position and M is the known motion or distance between any step. Our experiments were performed in a water tank.

$$\forall i = 1..N-1 : RA = |norm(q_i - q_{i+1}) - M| \tag{4}$$

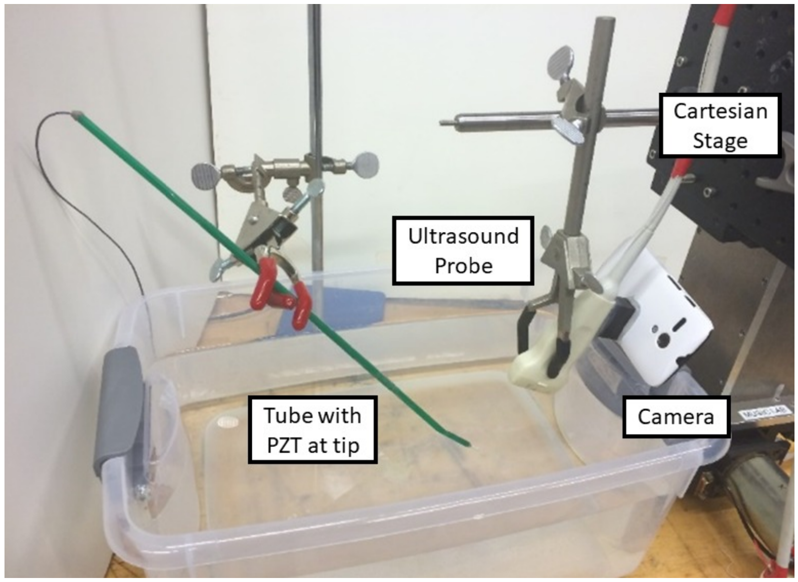

Figure 3. Experimental setup with a cartesian stage, a camera, and ultrasound probe, and the piezoelectric element.

4. Results

The first experiment resulted in errors of 0.63mm and 0.18mm on two independent poses. In the second experiment, this approach was used to compute the piezoelectric element location for each of the Cartesian stage configurations. Figure 4 represent subsets of the computed points with respect to the ultrasound image plane. As one can see, the computed points look like the three axes of motion applied using the Cartesian stage. Quantitatively, the relative accuracy measure described in equation 4 had a minimum, maximum, mean, and standard deviation of 0.02mm, 2.15mm, 0.61mm, and 0.61mm respectively.

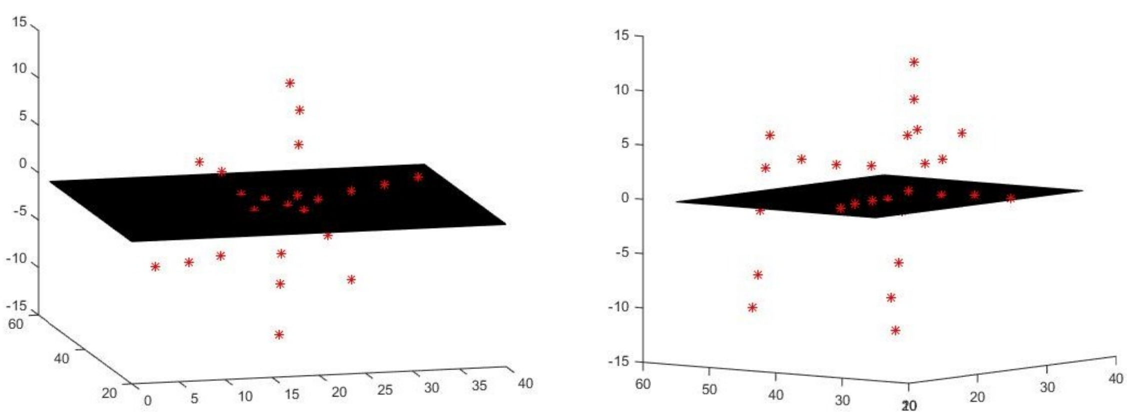

Figure 4. Subsets of detected PZT positions with respect to the ultrasound image plane (black plane).

5. Discussion

While the results from the experiments are promising, there are several extensions that must be made to improve the practicality of this method. First of all, these experiments were performed with a fabricated tool and not a real needle. Changing to a needle will require development to the camera segmentation methods. This method also relies on a strong assumption that there is no needle bending, at least not outside of the camera-needle plane. Any needle bending will result in errors to the needle tip estimation. This assumption is unlikely to hold, especially when the needle punctures tissue. One possible solution to this may to be add additional PZT sensors to the needle shaft to reduce the uncertainty of the needle's trajectory within the tissue.

6. Conclusion

In this work, we demonstrated the use of sensor fusion to track a piezoelectric element with two incomplete sources of sensor information. Through experiments performed in an ideal environment, on average, sub-millimeter errors were achieved. Future work will focus on demonstrating this method in more realistic *ex vivo* scenarios and explore whether our listed assumptions hold.

Acknowledgements

Financial support was provided by Johns Hopkins University internal funds, NIBIB-NIH grant EB015638: Interventional PhotoAcoustic Surgical System (i-PASS), NSF Grant No. IIS-1162095: Automated Calibration of Ultrasound for Image-Guided Surgical Procedures, NIGMS-/NIBIB-NIH Grant No. 1R01EB021396: Slicer+PLUS: Point-of-Care Ultrasound, NSF Grant No. IIS-1653322: Co-Robotic Ultrasound Sensing in Bioengineering, and NSH SCH:CAREER Grant 1653322.

References

1. Wood B.J., Zhang H., Durrani A., Glossop N., Ranjan S., Lindisch R.T., Levy E., Banovac F., Borgert J., Krueger S., Kruecker J., Viswanathan A., and Cleary K., "Navigation with Electromagnetic Tracking for Interventional Radiology Procedures", in Journal of Vascular and Interentional Radiology, 16(4), pp 493-505, 2005.
2. Stoll J., and Dupont P., "Passive markers for ultrasound tracking of surgical instruments", in Duncan J.S., Gerig G. (eds) Medical Image Computing and Computer Assisted Interventions – MICCAI 2005. Lecture Notes in Computer Science, 3750, Springer, Berlin, Heidelberg, pp. 41-48, 2005.
3. Okazawa S.H., Ebrahimi R., Chuang J., Rohling R.N., and Salcudean S.E., "Methods for segmenting curved needles in ultrasound images", in Medical Image Analysis, 10(3), pp. 330-342, 2006.
4. Cheung S., and Rohling R.N., "Enhancement of needle visibility in ultrasound guided percutaneous procedures", in Ultrasound in Medicine and Biology, 30(5), pp. 617-624, 2004.
5. Guo X., Kang H.J., Etienne-Cummings R., and Boctor E.M., "Active ultrasound pattern injection system (AUSPIS) for interventional tool guidance", in PLoS One, 9(10), 2014.
6. Duda R.O., and Hart P.E., "Use of Hough Transformation to Detect Lines and Curves in Pictures", in Communications of the ACM, 15(1), pp. 11-15, 1972.
7. Cheng A., Guo X., Zhang H.K., Kang H.J., Etienne-Cummings R., and Boctor E.M., "Active phantoms: a paradigm for ultrasound calibration using phantom feedback", in Journal of Medical Imaging 4(3), 035001, 2017.